ELSEVIER

Journal of Power Sources 64 (1997) 123–129

JOURNAL OF POWER SOURCES

Study of resistance changes related to premature capacity loss in lead battery plates

M. Calábek [a], K. Micka [b,*], P. Bača [a], P. Křivák [a], V. Šmarda [a]

[a] *Technical University of Brno, 662 09 Brno, Czech Republic*

[b] *J. Heyrovský Institute of Physical Chemistry, Academy of Sciences of the Czech Republic, 182 23 Prague 8, Czech Republic*

Abstract

Measurements of the resistance of the active material and of the interphase between the active material and the lead grid were performed by an exact d.c. method during cycling under two different regimes using specially prepared positive test electrodes with grids from seven different lead alloys. The results were compared with those obtained earlier by using a higher (1 h) discharge rate. In both cases, the premature capacity loss was caused by a low charging rate and it was related with increasing resistance of the active material, although the cycle life was distinctly longer at the lower (4 h) rate of discharge. The interphase resistance values of the individual ribs show a scatter which becomes very pronounced at the end of the cycle life, indicating a degradation of the porous electrode structure, often manifested by shedding of the active material.

Keywords: Premature capacity loss; Resistance; Lead/acid batteries; Positive plates

1. Introduction

The so-called premature capacity loss (PCL) of positive lead/acid battery plates, which is particularly appreciable with low-antimony or non-antimonial grid alloys, can have, in principle, two main causes: (i) formation of barrier layers at the grid-active mass interface (PCL-1), and (ii) increasing resistivity of the active mass (PCL-2) [1]. Both the contact resistance (resistance of the corrosion layer, interphase resistance) and the active mass resistance can be measured in situ exactly during charge/discharge cycling by our method using specially prepared positive test electrodes [2].

The present work is a continuation of our previous studies [2], where the test electrodes were cycled under two different regimes and discharged at about 1 h rate, approaching the regime in electric vehicles. For physical reasons (regarding current conduction parallel to the plate surface) the laboratory electrodes were made relatively thick (6–7 mm). The faradaic current distribution in porous electrodes is, in general, the more non-uniform the thicker are the electrodes [3], the conversion of the active material decreasing from the plate surface toward the lead grid. Experimental evidence for this phenomenon was obtained, with the mentioned laboratory electrodes, in our earlier work [4]. The non-uniform current distribution may affect the results of measurement of the contact resistance, while the measured active material resistance corresponds to some average through the cross section of the plate. In the present work, therefore, a lower, 4 h discharge rate was used, ensuring a more uniform current distribution in the pores.

2. Experimental

The measurements were carried out on test electrodes with collectors from pure lead and seven different lead alloys (Table 1). The preparation of the pasted test plates and the method of measurement were described in detail in Refs. [2,5]. The test electrodes were arranged into two groups differing by the charge regime, eight electrodes each, with

Table 1
Composition (in wt.%) of the lead grid alloys used

Grid type	Ca	Sb	Sn
Pb–Ca	0.09		
Pb–Ca–Sn-1	0.09		0.32
Pb–Ca–Sn-2	0.09		0.70
Pb–Sb-1		1.61	0.37
Pb–Sb-2		1.68	0.05
Pb–Sb-3		2.19	0.20
Pb–Sb-4		5.73	0.27

* Corresponding author.

PII S0378-7753(96)02512-8

differing grid composition. One group was cycled under a 'bad' regime and the other under a 'good' one [2,5,6]. In the bad regime, the charging current was adjusted so that the charge passed after 18 h was equal to 150% of that obtained after discharge in the previous cycle. In the good regime, the electrodes were charged more rapidly with a current of 0.5 A until the cell voltage reached 2.4 V, and then with a current of 0.25 A so that the total charge acquired was 125% of that obtained during discharge. The electrodes were discharged once a day at a current of 0.5 A ($C_{10}/4$, i.e. about 4 h discharge rate) to a cut-off voltage of 1.6 V (100% depth-of-discharge). In view of the slow changes of the measured resistances with the time [7], it was essential to keep regularity in the time schedule of measurements. The test cells were kept in a thermostat at 35 °C.

In the course of the resistance measurements during cycling, average values of the contact resistance, R_k, of the eight measured ribs of each electrode were determined, together with average values of the active mass resistance, R_m, of the seven sections between them. These values were obtained by the difference method either before the beginning of discharge (at least 3 h after the end of charging) or immediately after the end of discharge. Since the increase in resistance close to the end of the cycle life was often very large, it was considered more suitable to plot values of conductance, rather than resistance, i.e. $G_k = 1/R_k$, $G_m = 1/R_m$.

3. Results and discussion

Typical dependences of the discharge capacity, C, the mean interphase conductance, G_k, and the mean active mass conductance, G_m, on the cycle number under both the good and the bad cycling regimes are shown in Figs. 1 and 2 for electrodes with non-antimonial grids and in Figs. 3 and 4 for electrodes with antimonial grids. (More diagrams were

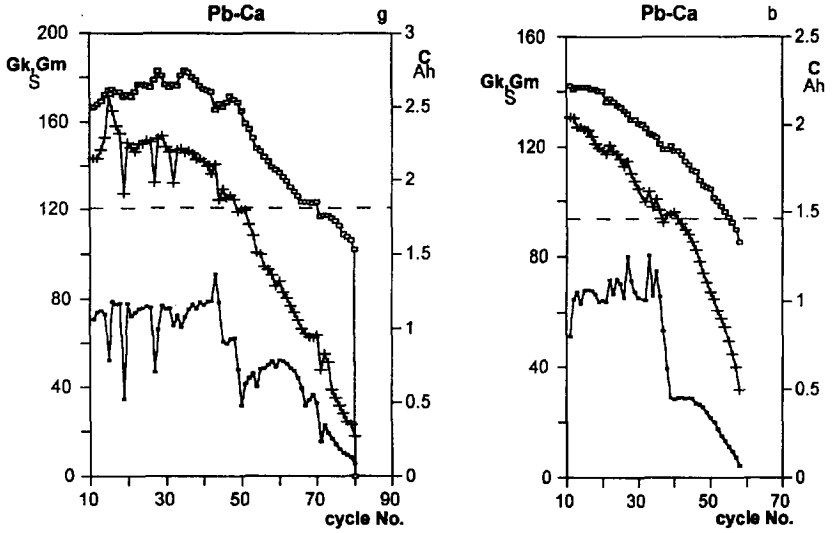

Fig. 1. Dependence (from the bottom to the top) of contact conductance, G_k, active mass conductance, G_m, and discharge capacity, C, on the cycle number for the electrode with a Pb–Ca collector cycled under the (g) good regime and (b) bad regime.

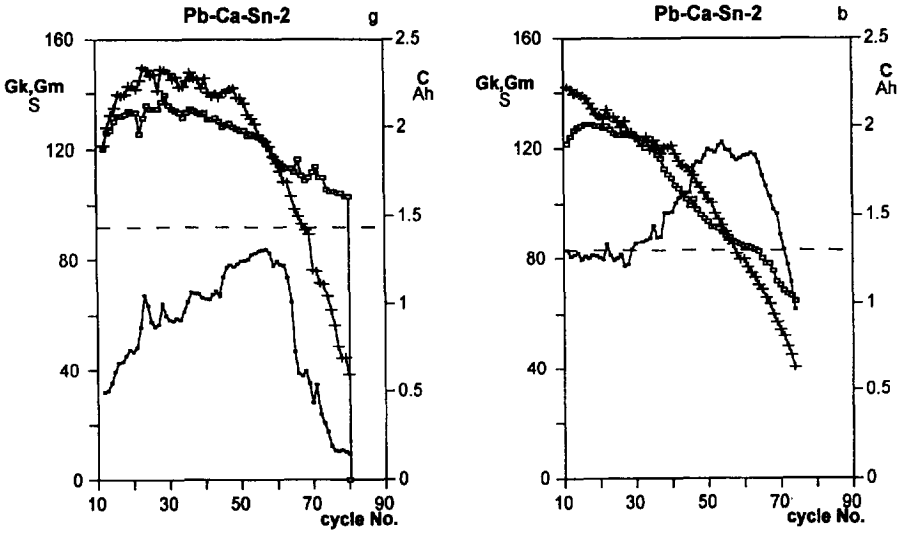

Fig. 2. Dependence of contact conductance, G_k, active mass conductance, G_m, and discharge capacity, C, on the cycle number for the electrode with a Pb–Ca–Sn-2 collector cycled under the (g) good regime and (b) bad regime.

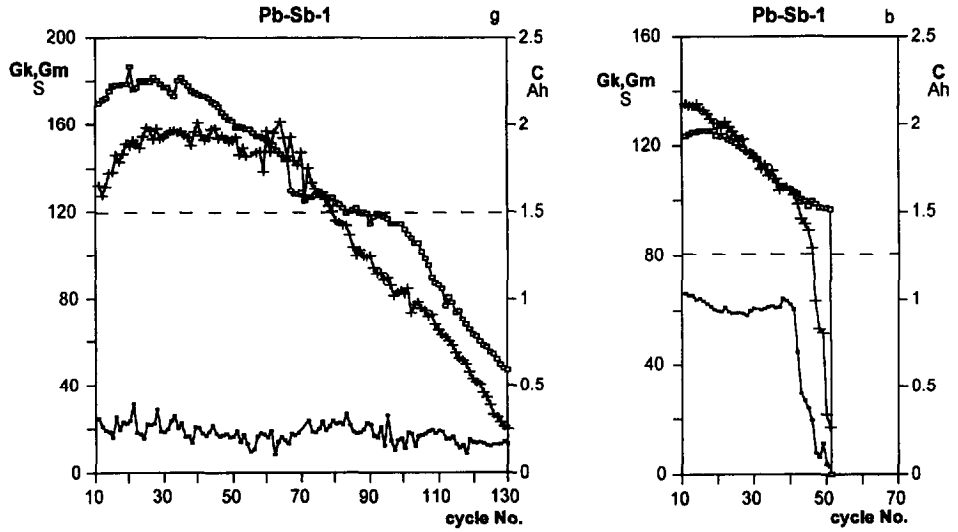

Fig. 3. Dependence of contact conductance, G_k, active mass conductance, G_m, and discharge capacity, C, on the cycle number for the electrode with a Pb–Sb-1 collector cycled under the (g) good regime and (b) bad regime.

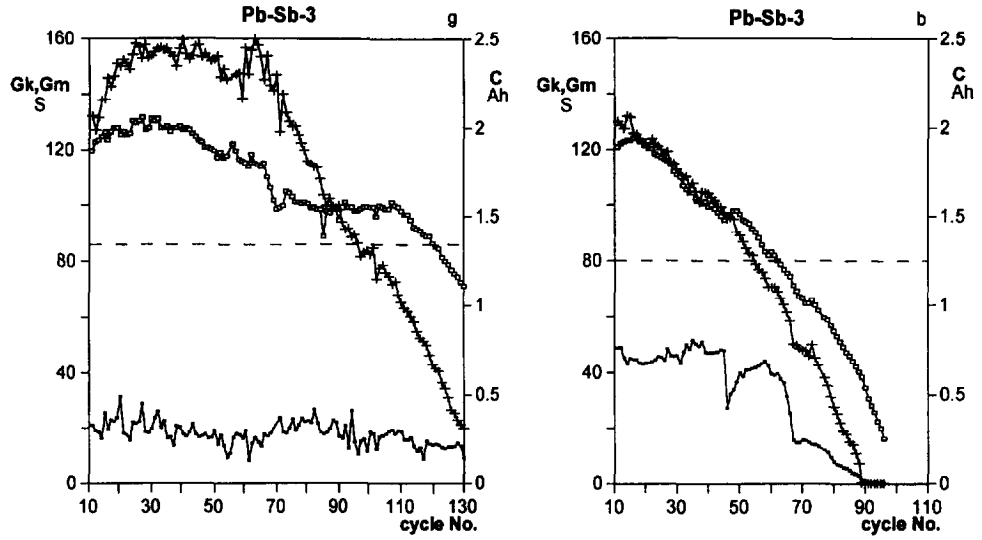

Fig. 4. Dependence of contact conductance, G_k, active mass conductance, G_m, and discharge capacity, C, on the cycle number for the electrode with a Pb–Sb-3 collector cycled under the (g) good regime and (b) bad regime.

included in our recent report [8].) The horizontal dashed line indicates 66% of the maximum discharge capacity, which was considered as the end of the cycle life. The conspicuous decrease of the capacity is an obvious manifestation of the PCL effect caused by the bad cycling regime. In contrast to our earlier work using a higher rate of discharge, electrodes with pure-lead and Pb–Ca grids now attained a rather high cycle life. At the end of the cycle-life test, shedding of the active material was often observed (causing the drop of G_m values), but the current collectors were not deteriorated.

3.1. Active material conductance

There is no clear correlation between the G_m values and the composition of the grid alloy. Somewhat lower values (about 80–110 S between the 10th and 20th cycles) were found for pure-lead grids [2] and, to some extent, also for the Pb–Sb-4 alloy. The results are summarized in Table 2. Although tin has no apparent influence on the initial G_m values, it retards their decrease with cycle number under the good regime, which is probably related with a moderate

Table 2
Approximate values of G_m (in S) from the 10th to the 20th cycles. Trend: (+) increasing, (−) decreasing, (+ −) oscillating; 4 h discharge rate

Grid type	G_m (good regime)	Trend	G_m (bad regime)	Trend
Pb	80–105	+ −	110–95	−
Pb–Ca	130–170	+ −	130–120	−
Pb–Ca–Sn-1	135–150	+	130–110	−
Pb–Ca–Sn-2	120–145	+	140–130	−
Pb–Sb-1	130–150	+	135–130	−
Pb–Sb-2	115–130	+	125–115	−
Pb–Sb-3	130–150	+	130–120	−
Pb–Sb-4	105–125	+	120–110	−

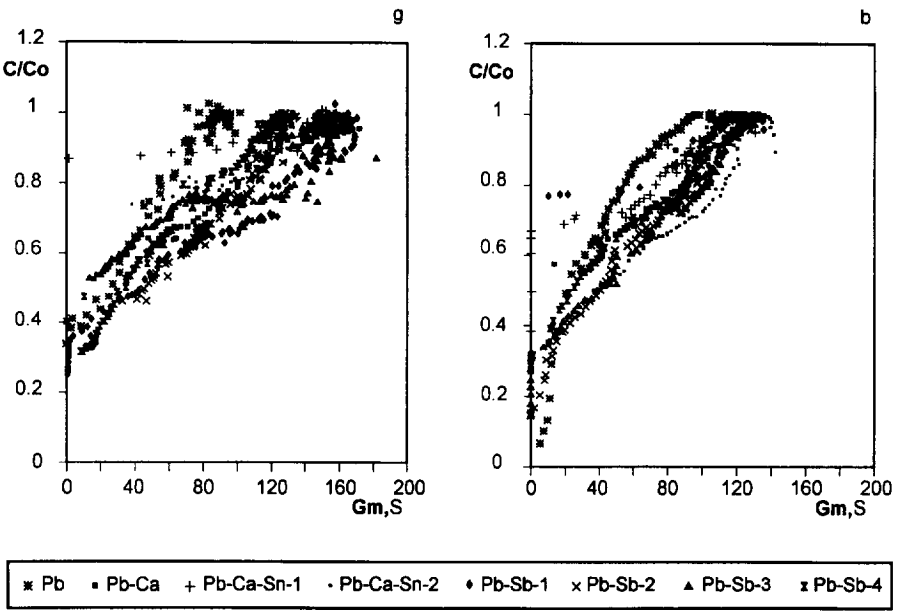

Fig. 5. Dependence of the normalized capacity, C/C_0, on the active mass conductance, G_m, measured in the charged state for electrodes with different collectors cycled under the (g) good regime and (b) bad regime; C_0 denotes the value of C in the 7th cycle.

increase in cycle life. This may be due to traces of tin leached out from the grid during cycling; a positive influence of tin on the conductivity of lead oxides was observed by many authors [9–11]. However, the behaviour of G_m depends substantially on the cycling regime: whereas under the good (rapid charging) regime the value of G_m shows an increasing (or, at least, oscillating) trend during the first 10–20 cycles, under the bad (slow charging) regime it always has a decreasing trend. This phenomenon was discussed by Winsel et al. [6], Meissner and co-workers [12,13] on the basis of their 'agglomerate of spheres' model, which takes into account the electric resistance of the 'necks' connecting the particles of lead dioxide.

The correlation between the values of G_m in the charged state and the discharge capacity, C, under the bad regime (Fig. 5) is similar to that found in our earlier work using the 1 h discharge rate [2,14]. Some related findings were reported already earlier [6,15]. However, under the good cycling regime, a significant influence of the grid composition is apparent at both discharge rates used. The decrease of the active material conductance with the cycle number is doubtless related with the decrease of its apparent density, reported already by Dittmann and Sams [16] and manifested by increasing plate thickness [17–19], i.e. decreasing mechanical strength. The decrease of G_m in the *discharged* state is much more profound. Hence, the influence of G_m in the *charged* state on the value of C is, in substance, an indirect one, and the correlation is rather weak.

The results obtained in our earlier work using 1 h discharge rate [2,14] were different in that the decrease of G_m values with the cycle number was more rapid, in agreement with the theory of Winsel et al. [6], according to which the 'necks' connecting the lead dioxide particles are more rapidly disrupted at higher discharge currents. Thus, in this case, the trend is more or less decreasing even under the rapid charging regime, and even more under the slow one (cf. Table 3). This behaviour, together with the failure of the pure-lead grid in the both regimes and of the Pb–Ca grid in the good regime, shows that the 1 h discharge rate represents a severe condition for the test electrodes.

Table 3
Approximate values of G_m (in S) from the 7th to the 17th cycle. Trend: always decreasing; 1 h discharge rate; data based on diagrams in Refs. [2,14]

Grid type	G_m (good reg.)	G_m (bad reg.)
Pb–Ca	95–55	140–100
Pb–Ca–Sn-1	115–100	130–90
Pb–Ca–Sn-2	160–120	120–80
Pb–Sb-1	160–130	120–80
Pb–Sb-2	110–90	100–65
Pb–Sb-3	95–80	130–90
Pb–Sb-4	125–115	130–90

On the whole, it can be said that the G_m values measured in the charged state are indicative of the 'health' or mechanical strength of the porous electrode, which becomes gradually worse during deep-cycling. This leads to a parallelity between the decrease of the capacity and of the active mass conductance, although the influence of the grid composition interferes.

3.2. Interphase conductance

The lowest values of G_k (at the 10th to 20th cycles) were measured under the good regime with pure-lead grids, namely below 10 S, and with the Pb–Sb-1 through Pb–Sb-4 grids, around 20 S. Similarly, low values of G_k with antimonial lead grids under the good regime were found in our preceding work employing a higher discharge rate [1]. Under the bad

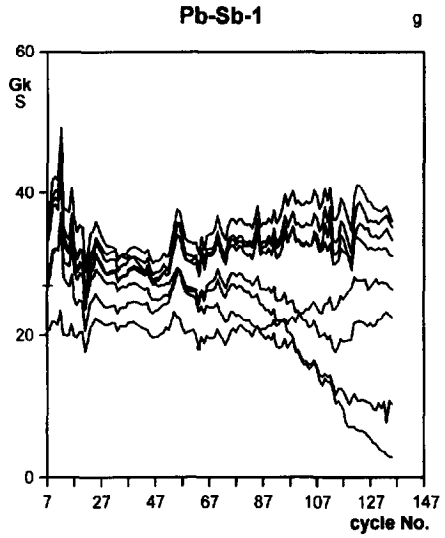

Fig. 6. Dependence of the contact conductance, G_k, on the cycle number for individual Pb–Sb-1 collector ribs measured under the good regime using 1 h discharge rate.

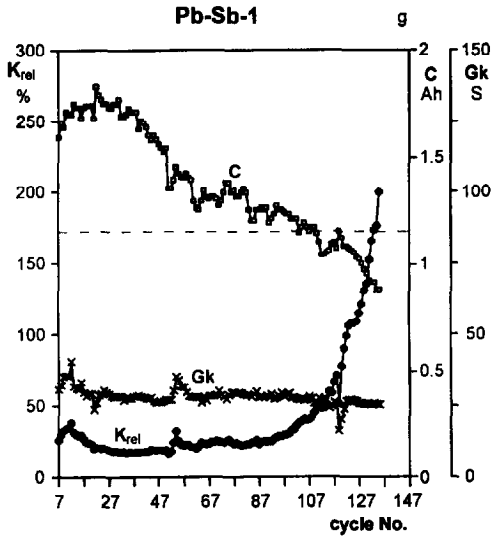

Fig. 7. Dependence of the criterion K_{rel}, corresponding to Fig. 6, together with the contact conductance, G_k, and discharge capacity, C, on the cycle number.

regime or with the other grid alloys under either regime, the corresponding G_k values ranged from 40 to 80 S, except for the Pb–Ca–Sn-2 grid under the bad regime, where they ranged from 80 to 120 S (Fig. 2). It is noteworthy in this respect that Simon et al. [11] observed a positive influence of tin on the conductance of the oxide layer on the lead grid only at a tin content of 0.8–1.5%, which was approached by the composition of the Pb–Sn-2 grid. The influence of tin on the G_k values is not unambiguous; it was not observed under the good cycling regime, see also [2,8,14]. The resulting moderate increase of the cycle life is probably related with the effect on G_m mentioned in Section 3.1. The development of the interphase conductance has nothing to do with the limit of the cycle-life test defined by the horizontal dashed line in Figs. 1 to 4. The abrupt fall of some curves is due to plate disintegration.

In spite of the conspicuous differences in G_k values, the discharge curves for the particular test electrodes were very similar, so that they partly (at least in their initial course) overlapped. Indeed, if one rib has an interphase conductance G_k, the value for the whole electrode is equal to $10G_k$ and the ohmic voltage drop $IR = 0.1I/G_k$, where I denotes the discharge current. In our case, $I = 0.5$ A, and for $G_k = 10$ S we obtain $IR = 0.005$ V, a negligible value. On the other hand, in our previous work [5] we obtained for a pure-lead grid $G_k = 0.25$ S in the fourth cycle at $I = 1.25$ A, hence $IR = 0.50$ V, which indeed corresponds to the observed shift of the discharge curve to lower voltage values. Thus, we conclude that the 'barrier layer model' of PCL-1 [1,20,21] may be applied to pure-lead grids, but not to alloyed lead grids.

The interphase (or contact) conductances illustrated in Figs. 1 to 4 are averages calculated from the arithmetic mean resistances for eight ribs. In reality, there is a considerable

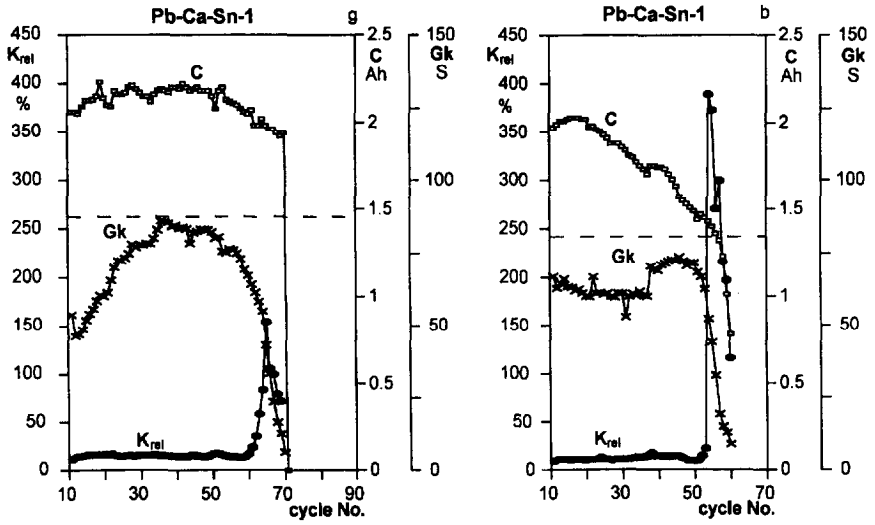

Fig. 8. Dependence of the criterion K_{rel} on the cycle number for electrode with the Pb–Ca–Sn-1 collector measured under the (g) good regime and (b) bad regime together with the contact conductance, G_k, and discharge capacity, C.

scatter [5], which can be characterized mathematically by the following criterion, K_{rel}

$$K_{rel} = \frac{1}{N\bar{R}_k}[\Sigma D_i^4]^{1/4} \quad (1)$$

where

$$\bar{R}_k = \frac{1}{N}\Sigma R_{ki}, \quad D_i = R_{ki} - \bar{R}_k \quad (2)$$

and N denotes the number of measured values of the resistances, R_{ki}, for individual ribs. This criterion, in contrast to the standard deviation, emphasizes larger deviations against smaller ones. For illustration, in Fig. 6 are shown the measured conductances for individual ribs of the Pb–Sb-1 grid, and in Fig. 7 the criterion K_{rel}, mean interphase conductance, and discharge capacity as functions of the cycle number (1 h discharge rate, good cycling regime).

To elucidate the question whether a large scatter of the R_{ki} values (causing possibly non-uniform current distribution over the plate surface) may shorten the cycle life of the positive electrode, the measured R_k data were treated by the above mathematical procedure and some results are presented graphically in Fig. 8. A considerable inhomogeneity of the interphase (contact) resistances, i.e. a high K_{rel} value, appears before the end of the cycle life mainly with Ca-containing grids (in total in eight cases), whereas it appears after the end of the cycle life with pure-lead or with animony-containing grids (for which $K_{rel} < 50\%$ during the whole cycle life).

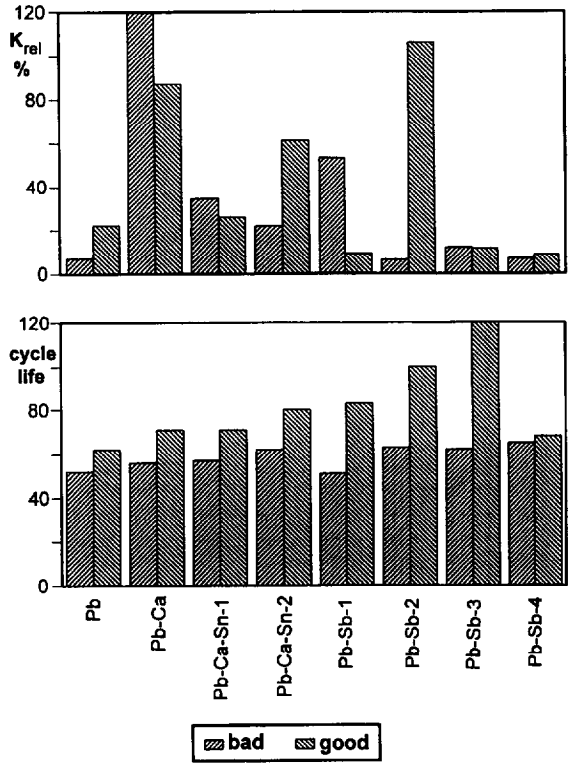

Fig. 9. Upper half: criterion K_{rel} averaged over the whole cycle life for electrodes with different collectors cycled under the good and under the bad regime at the 4 h discharge rate. Lower half: cycle life of electrodes with various grid alloy compositions cycled under the bad and under the good regimes (at 4 h discharge rate).

The data obtained earlier by discharging at the higher rate [2,14] were treated analogously and the results were similar. A substantial increase of the criterion K_{rel} was only observed in two cases before the end of the cycle life (in three cases not at all, in nine cases after the end). An overview of the results is shown in Fig. 9, where values of K_{rel} averaged over the whole cycle life are given for each electrode under either regime at the 4 h discharge rate, together with the cycle lives attained. A comparison of the two diagrams reveals no parallelity.

On the whole, it can be inferred that the steep rise in the inhomogeneity of contact conductances or resistances is not the cause of the electrode breakdown, but that these two phenomena have probably the same reason, i.e. degradation of the active material structure due to prolonged deep cycling. The measured G_k values are too high to cause an appreciable IR drop under the given conditions.

4. Conclusions

Exact conductance measurements on laboratory positive plates with grids from seven different lead alloys showed that the loss of capacity during cycling is associated with decreasing conductance of the active material. The interphase (contact) conductance either does not change appreciably during cycling or begins to drop only at the end of the cycle life. These findings are practically the same at a 4 h as at a 1 h discharge rate.

It was substantiated that a low charging rate (bad cycling regime) causes PCL (shortening of the cycle life), which becomes considerably alleviated when a lower (4 h) discharge rate is used, compared with the 1 h discharge rate.

Our results suggest that the 'active mass resistivity model' (PCL-2) is suitable for elucidation of the premature capacity loss of positive electrodes with alloyed lead grids, whereas the 'barrier layer model' (PCL-1) may be applied to positive electrodes with pure-lead grids.

Acknowledgements

This work was supported by the Advanced Lead–Acid Battery Consortium (in Project No. AMC-010), a program of the International Lead Zinc Research Organization, and by the Grant Agency of the Czech Republic.

References

[1] A.F. Hollenkamp, K.K. Constanti, A.M. Huey, M.J. Koop and L. Apăteanu, *J. Power Sources, 40* (1992) 125.

[2] M. Calábek, K. Micka, P. Bača, P. Křivák and V. Šmarda, *J. Power Sources, 62* (1996) 161.

[3] I. Roušar, K. Micka and A. Kimla, *Electrochemical Engineering*, II, Elsevier, Amsterdam, 1986.
[4] A.F. Hollenkamp, K.K. Constanti, M.J. Koop, L. Apăteanu, M. Calábek and K. Micka, *J. Power Sources, 48* (1994) 195.
[5] A.F. Hollenkamp, M. Calábek, P. Bača, K.K. Constanti, M.J. Koop, K. McGregor, K. Micka and V. Šmarda, *ALABC Projects Nos. AMC-003 and AMC-003A, Prog. Rep. No. 7 and No. 2, Oct.–Dec. 1994.* CSIRO Divsion Mineral Products, Melbourne, *Communication MPC/M-500*, Jan. 1995.
[6] A. Winsel, E. Voss and U. Hullmeine, *J. Power Sources, 30* (1990) 209.
[7] M. Calábek and K. Micka, *J. Power Sources, 30* (1990) 309.
[8] M. Calábek, K. Micka, P. Bača and V. Šmarda, *ALABC Project AMC-010, Prog. Rep. No. 1, Oct.–Dec. 1995*, Technical University of Brno, 662 09 Brno, Czech Republic, Febr. 1996.
[9] H. Döring, J. Garche, H. Dietz and K. Wiesener, *J. Power Sources, 30* (1990) 41.
[10] R.T. Barton, P.J. Mitchell and F.A. Fleming, *Power Sources, 13*, 1991, p. 25; *Chem. Abstr., 118*, (1993) 208, Abstr. No. 184 306v.
[11] P. Simon, N. Bui and F. Dabosi, *J. Power Sources, 50* (1994) 141.
[12] E. Meissner and E. Voss, *J. Power Sources, 33* (1991) 231.
[13] E. Meissner and H. Rabenstein, *J. Power Sources, 40* (1992) 157.
[14] M. Calábek, K. Micka, P. Bača and V. Šmarda, *ALABC Project No. AMC-003A, Prog. Rep. No. 3, Jan.–Mar. 1995*, Technical University of Brno, 662 09 Brno, Czech Republic, Apr. 1995.
[15] K. Takahashi, M. Tsubota, K. Yonezu and K. Ando, *J. Electrochem. Soc., 130* (1983) 2144.
[16] J.F. Dittmann and J.F. Sams, *J. Electrochem. Soc., 105* (1958) 553.
[17] K. Micka, M. Svatá and V. Koudelka, *J. Power Sources 4* (1979) 43.
[18] D. Pavlov and E. Bashtavelova, *J. Electrochem. Soc. 133* (1986) 241.
[19] S. Atlung and B. Zachau-Christiansen, *J. Power Sources, 30* (1990) 131.
[20] M.K. Dimitrov and D. Pavlov, *J. Power Sources, 46* (1993) 203.
[21] D. Pavlov, *J. Power Sources, 48* (1994) 179.